SAE 2023-01-1662

Comparing Real Driving Emissions from Euro 6d-TEMP Vehicles Running on E0 and E10 Gasoline Blends

Varun Shankar[a], Ime Usen[b], Nick Molden[b], Christopher Willman[a], Felix Leach[a]*
[a] Department of Engineering Science, University of Oxford, Oxford, United Kingdom
[b] Emissions Analytics, High Wycombe, Buckinghamshire, United Kingdom

ABSTRACT

Several governments are increasing the blending mandate of renewable fuels to reduce the life-cycle greenhouse gas emissions of the road transport sector. Currently, ethanol is a prominent renewable fuel and is used in low-level blends, such as E10 (10 %v/v ethanol, 90 %v/v gasoline) in many parts of the world. However, the exact concentration of ethanol amongst other renewable fuel components in commercially available fuels can vary and is not known.

To understand the impact of the renewable fuel content on the emissions from Euro 6d-TEMP emissions specification vehicles, this paper examines the real-driving emissions (RDE) from four 2020 to 2022 model-year vehicles run on E0 and E10 fuels. CO, CO_2, NO, and NO_2 were measured through a Portable Emissions Measuring System (PEMS). In addition, N_2O, formaldehyde, acetaldehyde, volatile organic compounds (VOCs), and other gaseous and particulate tailpipe emissions were measured and categorized in cold-start, urban, rural, and motorway segments with a proprietary system developed by Emissions Analytics. Engine-out emissions were also measured from a single-cylinder engine at steady-state low speed and load conditions.

The results show that the aldehydes, VOCs, and N_2O emissions were greatest at cold-start and lowest at motorway conditions. The formaldehyde real-driving emissions increased by 14 % on average between the E0 and E10 fuels. However, the formaldehyde engine-out emissions were reduced for E10. Acetaldehyde real-driving emissions were below the detectable threshold for both E0 and E10 fuels, whereas, engine-out emissions increased for the E10. Whilst CO emissions presented inconsistent results across the cars and driving conditions, a reduction in CO_2 emissions with the E10 fuel was observed across all conditions. NOx emissions increased for E10 compared to the E0 fuel in urban conditions and the opposite was observed for the motorway conditions. These findings highlight the need for the co-development of emissions regulations as greater ethanol and other renewable fuel content is blended into gasoline.

INTRODUCTION

Ethanol is widely used as an alternative fuel or an effective additive to gasoline as it can be produced sustainably from non-fossil feedstock and has advantageous combustion properties. As a result, many countries are implementing legislation to increase the use of ethanol. For example, in India, the 10 %v/v blending mandate of ethanol was met in 2022 and they have revised the 20 %v/v blending target to 2025 [1]. By 2030, the European Union (EU) aims to increase the share of renewable fuel in transport to at least 14 %v/v including a minimum share of 3.5 %v/v of advanced biofuels produced from non-food crop sources [2].

The effect of ethanol addition to gasoline has presented varied results on many regulated and unregulated emissions [3]. This is due to factors such as the fuel composition, the percentage of ethanol content, ambient conditions, exhaust gas flow velocity (residence time), and the vehicle's age, size, and emissions specification.

In addition to emissions testing in a laboratory on an engine test cell or vehicle on a chassis dynamometer, it is crucial to measure the emissions for representative real-driving conditions with a portable emissions measuring system (PEMS) [4]. Furthermore, an increasingly high proportion of emissions are produced during cold-start conditions, however, this may be underrepresented if it forms a small share of the official test cycle [5]. Whilst the PEMS can be used to detect emissions in real-time, the system is limited to certain pollutants such as NO, NO_2, CO, CO_2, and total hydrocarbons (THC). The latter encompasses hundreds of hydrocarbons without speciation and identification of volatile organic compounds, such as aldehydes. Therefore, a detailed understanding of the proportion of the emissions based on driving segmentation will inform the upcoming regulations of real-world conditions.

This study aims to investigate the use of improved real-driving emissions (RDE) measurements with a larger array of hydrocarbon speciation supplementing the traditional PEMS. This includes the identification of hazardous pollutants such as formaldehyde, acetaldehyde, acetone, acetic acid, benzaldehyde, toluene, and nitrous oxide (N_2O) which can be affected by blending ethanol in gasoline. These emissions (excluding N_2O) are often categorized as non-methane volatile organic compounds (NMVOCs). Studies have found that road transport contributes approximately 16 % of the atmospheric NMVOC emissions [6, 7]. More specifically in urban areas, Liu *et al.* [8] found road transport contributed to 33.8 % of the NMVOCs in Beijing, China, with two-thirds from gasoline vehicles and a third from diesel vehicles. Furthermore, oxygenated volatile organic compounds, such as formaldehyde and acetaldehyde, can represent around 40 % of the NMVOCs [7]. A survey of the literature findings on the impact of ethanol-gasoline blends on each of these emissions in addition to the regulated RDE such as NOx, CO, and CO_2 is performed. Understanding the emissions impact of upcoming alternative fuel blends is vital as road transport is responsible for around 24 % of the total CO_2 emissions in the EU [9] and the source of 58 % of the NOx emissions globally [10].

Formaldehyde - Formaldehyde is classified as a human carcinogen by the United Sated of America (USA) Department of Health

and Human Services [11]. Literature found that formaldehyde emissions are formed at more appreciable amounts with higher content (over 50 %v/v) of ethanol in gasoline [12–15]. Furthermore, the literature generally found that the rate of increase in formaldehyde emissions with ethanol content is not as significant as the acetaldehyde emissions [16, 17]. Yang *et al.* [18] reported that formaldehyde could also depend on the fuel's aromatic content. Clairotte *et al.* [14] found formaldehyde emissions to be enhanced at a higher temperature than acetaldehyde emissions.

Acetaldehyde - Cheng *et al.* [19] found that compared to conventional low-temperature branching pathways, ethanol favors OH radical scavenging pathways forming acetaldehyde and hydroperoxyl (HO_2) radicals. Therefore, acetaldehyde is primarily formed during ethanol's oxidation pathway explaining the tendency for acetaldehyde to increase with ethanol concentration [20]. Specifically at the low-temperature conditions found during the cold-start phase, the literature found a definite increase in acetaldehyde emissions with any quantity of ethanol addition to gasoline [12–17, 21–23].

Acetone - Exposure to acetone can affect the eyes and act as a skin irritant. At moderate to high level exposure, acetone can irritate the respiratory system and lead to headaches and light-headedness [24]. Sarathy *et al.* [20] highlight that acetone could be produced as a β-scission product of the parent alcohol fuel radicals. Dryer *et al.* associates direct acetone formation through the secondary radical reaction of iso-octane [25]. However, Poulopoulos *et al.* [26] found that whilst acetone engine-out emissions were increased for E10 at low engine loads, after the catalytic treatment, the acetone emissions were significantly decreased. In addition to aldehydes, the impact of low ethanol content in gasoline on exhaust acetone emissions needs to be monitored.

Acetic acid - Carboxylic acids (formic and acetic acids) can contribute to the acidity of gas and aqueous phases of the atmosphere [27]. These acids can be formed during combustion. The generation of acetic acid as an exhaust emission can be linked to the fuel composition. Battin-Leclerc *et al.* [27] and Zervas *et al.* [28] have found that the presence of aromatic compounds, such as toluene, in the fuel strongly influences the formation of acetic acid. Furthermore, they attribute the addition of the OH to CH_3CO radical reaction to contribute to acetic acid formation [29, 30]. As ethanol oxidation produces OH and oxygenated C_2 radicals, fuels with ethanol content could increase the acetic acid exhaust concentration.

Benzaldehyde - An aromatic aldehyde formed as an intermediate during combustion. At low concentrations, it has been reported as a skin irritant [31]. Generally, the major source of exhaust benzaldehyde emissions has been from fuel aromatic hydrocarbons, such as toluene [32–34]. The impact of blending ethanol in gasoline on benzaldehyde emissions has presented competing findings. Some authors found that fuels with low oxygenate content, such as E10, slightly enhance benzaldehyde formation as the aromatic oxidation improves [35, 36]. Dagaut *et al.* [32] found that for toluene, an aromatic, oxidation can occur by H-atom abstraction to form benzyl radicals which oxidize to benzaldehyde. The OH radicals from ethanol oxidation could initiate and propagate the H-atom abstraction. Nevertheless, Magnusson *et al.* [37] found that the formation of benzaldehyde from ethanol was negligible in ethanol-gasoline blends and not detectable from pure ethanol. The presence of low ethanol content in gasoline fuels with similar aromatic content could highlight ethanol's impact on exhaust toluene and benzaldehyde emissions.

Nitrogen oxides NOx - The traditional PEMS is capable of computing NOx which is composed of NO and NO_2 measurements. NO is a major constituent of NOx for gasoline SI engine vehicles. The impact of ethanol content in gasoline on NOx has varied results. Some literature shows that NOx emission decreases with increasing ethanol content in gasoline [3, 38–41]. They attribute this decrease in NOx emissions due to a reduction in peak in-cylinder temperature, resulting from combustion retardation, and the reduction in exhaust temperature, due to lower flame temperature. Masum *et al.* [42] found that increasing ethanol content inhibits the thermal NO reaction pathways leading to a decrease in NOx emissions. Zhang *et al.* [43] found a significant reduction in NOx emissions over the catalytic converter and associate this with the excess air coefficient of the blended ethanol-gasoline fuel. In contrast, literature also shows increased NOx emissions with ethanol-gasoline fuels [44, 45]. The higher heat release of ethanol and the increased oxygen content in the fuel-rich conditions are attributed to the increase in NOx emissions. With increasingly strict NOx emissions legislation, further evaluation of the Euro 6d-TEMP emissions stage vehicles with fuels that contain ethanol is required. Additionally, as O'Driscoll [46] found NOx emissions were higher during urban driving than the motorway, it is important to evaluate the real-driving NOx emissions at different driving conditions to understand the implications on public health.

Nitrous oxide N_2O - N_2O has been considered for regulation as it is an air pollutant and greenhouse gas (GHG) with a warming potential significantly greater than CO_2 [5]. N_2O is formed at low-temperature (110°C to 350°C) primarily during catalyst light-off [47, 48]. During this period, when a nitrogen atom encounters a molecule of NO on the surface, as the catalyst has not reached a sufficient temperature to completely reduce the NOx, a molecule of N_2O can be formed and released [49]. Graham *et al.* [50] found that cold engine start and congested urban driving, which have cooler exhaust temperatures result in increased N_2O emission rates. Wang *et al.* [51] found that N_2O can also be formed by the reduction of NO by alkanes at higher temperatures and aging catalysts take a longer time to warm up, which favors the formation of N_2O. The formation of N_2O at different driving segments with modern vehicles would aid the understanding in developing ways to curb the emissions.

Carbon monoxide CO - CO is a GHG emission and the effect of ethanol in gasoline has been previously studied. Suarez-Bertoa *et al.* [52] found an increase in CO emissions at cold ambient temperature and associate this with the use of rich air-fuel mixtures at cold-starts, incomplete combustion close to the cold cylinder walls, low catalytic efficiency, and longer periods to reach catalyst light-off temperature. Despite testing fuels with increasing ethanol concentration, they found CO emissions are similar across the fuels over the drive cycle, which is consistent with previous findings [12, 16, 52]. However, Zhang *et al.* [43] found that the CO emissions decreased with increasing ethanol content in gasoline as the oxygen content in the fuel increases enabling more complete combustion and easier oxidation of the CO. Therefore, further evaluation on the formation of CO at different driving segments for fuels with and without ethanol will be helpful.

Carbon dioxide CO_2 - Suarez-Bertoa *et al.* [41] found no statistically significant trend as a consequence of ethanol content ranging from 5 to 15 %v/v in gasoline. Nevertheless, Jin *et al.* [15] reported that the adoption of E10 (10 %v/v ethanol in gasoline) had resulted in a reduction of CO_2 emissions.

With increasing ethanol content in gasoline driven by government mandates, identifying the concentrations of the individual species across a standardized real-driving emissions test with known fuel compositions (with and without ethanol) will be effective to develop methods to control their emissions. Emissions Analytics have developed a practical method for measuring and identifying these hydrocarbon compounds and VOCs in real-world conditions to understand their importance for future regulations [5]. They are also able to measure regulated pollutants through the traditional PEMS. Therefore, this work explores the impact of ethanol addition to gasoline on regulated and unregulated emissions. Two EN228-compliant [53] fuels, E0 (0 %v/v

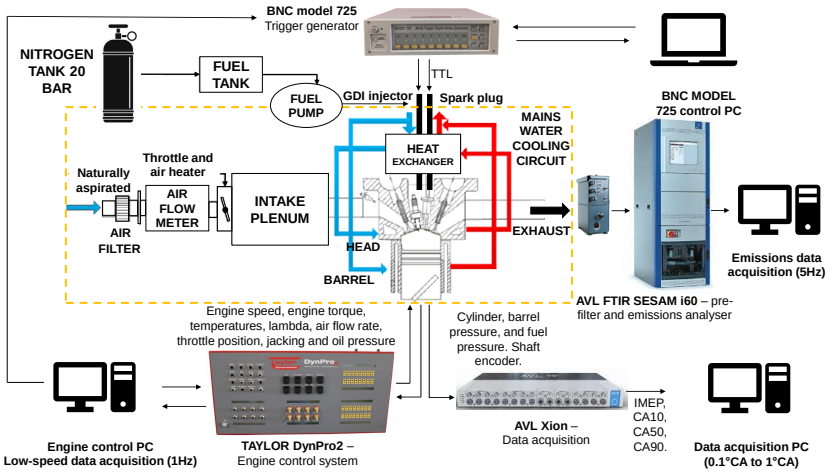

Figure 1: Single cylinder engine configuration.

ethanol) and E10 (10 %v/v ethanol), of known composition were blended. They were tested on four vehicles with Euro 6d-TEMP emissions specification with real-driving emissions measured on the EQUA™ test programme using the PEMS and proprietary VOCs system. The fuels were also tested on a single-cylinder gasoline direct injection (GDI) spark ignition (SI) engine in a laboratory at low speeds and loads with engine-out emissions measured in real-time (1 Hz) using Fourier transform infrared spectroscopy (FTIR). Aldehydes and alcohols up to C_7 including formaldehyde and acetaldehyde, acetone, acetic acid, benzaldehyde, toluene, N_2O, NO_x, CO, and CO_2 were evaluated for both fuels.

EXPERIMENTAL SETUP

For this work, emissions measurements were performed on a laboratory-based engine and onboard vehicles on the road.

SINGLE CYLINDER ENGINE

For the laboratory-based experiments, a single-cylinder engine was used. The configuration is shown in Figure 1. This engine may be configured for optical access, but a non-optical piston and barrel were used as optical access was not required. The Taylor DynPro2 controlled the test cell and Control Techniques dynamometer which regulated the engine torque and speed. For combustion, the fuel was injected at a pressure of 150 bar and a centrally mounted spark plug ignited the mixture. Injection and ignition timing and injection duration were controlled by the Berkeley Nucleonics Corporation (BNC) model 725 unit using trigger signal inputs from the shaft encoder. An oil-free combustion system was adopted, so that the emission impacts can be attributed directly to the fuel and operating conditions. Polyamide-imide piston rings were used and the engine coolant was maintained at 45 °C to reduce the risk of melting the rings. K-type thermocouples were used to measure all temperatures. This facility has been extensively described in previous work [54].

Table 1: Single cylinder engine specifications and settings.

Parameter	Unit	Value
Bore	mm	89.0
Stroke	mm	90.3
Displacement	cm^3	562
Compression ratio	-	11:1
Fuel pressure	bar	150
Valves per cylinder	-	2 intake; 2 exhaust
Injection timing	°CA aTDC	-270
Ignition timing	°CA aTDC	-46.3

Low-speed data, such as exhaust temperature, was recorded at 1 Hz by the Taylor DynPro2 system, whilst high-speed data, such as the cylinder pressure measured using a Kistler Type 6041A pressure transducer, was logged using the AVL X-ion high-speed data acquisition system at 0.1 °CA resolution. The load, represented as the indicated mean effective pressure (IMEP), was calculated using the cylinder pressure data. Once the engine reached stable operation, three independent runs were conducted at each operating point with high-speed data for 300 cycles of each run measured. A lambda sensor, placed at the exhaust of the engine, was used to measure the fuel-air equivalence ratio (ϕ) and was calibrated in free air. For the E0 and E10 fuels, stoichiometry was assumed at 14.7 and 14.1, respectively. The specifications of the engine are presented in Table 1.

The emissions were measured in real-time (sampling rate of 5 Hz) using a Fourier transform infrared spectroscopy (FTIR) gas analyzer (AVL SESAM FTIR i-60). The exhaust sample line was maintained at 191 °C and 800 hPa to enable effective gas transfer. The sample flow rate was maintained at 8 L/min through the 200 mL gas cell. Prior to each operating condition and fuel change, the background spectrum which determines the absorbance was normalized by purging inert nitrogen gas through the gas cell. The high operating temperature of the gas cell (191 °C) enabled the FTIR gas analyzer to sample the raw exhaust without contamination of the optics with water vapor and emission constituents. Upstream, the sample line was also heated to 191 °C preventing losses from adsorption and condensation. A heated filter removed particulate matter before the sample entered the heated line to prevent optical cell contamination. The filter was renewed for each of the fuels tested. The specifications of the measured emissions presented in this study can be found in Table 2. The total nitrogen oxides (NOx) was calculated as a sum of nitrogen monoxide (NO) and dioxide (NO_2). The values in Table 2 identify the detection range of the emission species in this study and the accuracy defines the nominal accuracy of each of the species within the detectable range.

Table 2: FTIR emissions specifications relevant to this study.

Emission component	Formula	Unit	Range	Accuracy
Formaldehyde	HCHO	ppm	0-1000	± 0.15
Acetaldehyde	CH_3CHO	ppm	0 - 3000	± 0.35
Nitrogen monoxide	NO	ppm	0 - 10000	± 0.15
Nitrogen dioxide	NO_2	ppm	0 - 1000	± 0.06
Nitrous oxide	N_2O	ppm	0 - 1000	± 0.05
Carbon monoxide	CO	ppm	0 - 100000	± 0.1
Carbon dioxide	CO_2	ppm	0 - 200000	± 10.0

REAL DRIVING EMISSIONS

On-road tailpipe exhaust emissions were measured by Emissions Analytics using SEMTECH-LDV Portable Emissions Measurement System (PEMS) developed by Sensors Inc [55]. The measurement accuracy and linearity of the SEMTECH-LDV PEMS satisfy the European Union (EU) and the United States of America (USA) emissions testing requirements and are within the range of laboratory testing [56–58].

The SEMTECH-LDV PEMS unit (Figure 2) was equipped with a tailpipe attachment, heated exhaust lines, a range of gas analyzers, a Global Positioning System (GPS) receiver, a weather station for ambient measurement, and an interface with the vehicle's on-board diagnostics [57]. A non-dispersive infrared sensor was used to measure the carbon monoxide (CO) and carbon dioxide (CO_2), whereas a non-dispersive ultraviolet sensor was used for nitrogen monoxide and dioxide which were summed to calculate the nitrogen oxides (NOx) concentration [55]. All the gaseous emissions were recorded at 1 Hz. The GPS receiver recorded vehicle speed, longitude, latitude, and altitude [46]. The engine operation was not affected by the PEMS as it was powered by batteries and the additional weight of the PEMS was uniform for each test. This additional weight may have affected the test vehicle's power-to-mass ratio and previous results have found a potential increase in CO_2 emissions by up to 3% [56]. Further detail on the PEMS installation and SEMTECH-LDV operation can be found in the literature [57, 59].

Figure 2: SEMTECH-LDV portable emissions measuring system (PEMS) (left) and an example vehicle with the PEMS experimental measurement set-up (right).

The concentrations of volatile organic compounds (VOCs), semi-VOCs, hydrocarbons with two carbon atoms up to at least forty-four carbon atoms (C_2 to C_{44}), formaldehyde (CH_2O), nitrous oxide (N_2O), and many others were measured using an innovate patent-pending system by Emissions Analytics [5, 60]. This proprietary VOCs system sampled real-driving exhaust emissions onto tubes (Figure 3) which were subsequently analyzed using gas chromatography in a laboratory. A two-dimensional gas chromatography (GCxGC) system coupled with a time-of-flight mass spectrometer (TOF-MS) from SepSolve Analytical (UK) and Markes International (UK) was used [61, 62]. The identification and quantification of the compounds were enabled by the TOF-MS and supported by other detectors such as flame ionization detector (FID) and electron capture detector (ECD) for nitrous oxide (N_2O). Formaldehyde (CH_2O) was analyzed by the 1220 Infinity II high-performance liquid chromatography (HPLC) technique provided by Agilent [63].

The system could simultaneously sample onto multiple tubes with distinct characteristics. For formaldehyde (CH_2O), the tubes contained a 2,4-dinitrophenylhydrazine (2,4-DNPH) cartridge which transformed CH_2O into a stable form for complete capture, whereas, for N_2O, the tubes had a molecular sieve. This approach enabled the identification and collection of a wide spectrum of measured compounds with a high degree of sensitivity thus picking up species with low concentrations.

Coupled with the PEMS unit that had exhaust flow rate and GPS data, the concentration of the measured VOCs was converted

Figure 3: Thermal desorption tube from Markes International (left) and two-dimensional gas chromatography (GCxGC) system coupled with a time-of-flight mass spectrometer (TOF-MS) from SepSolve Analytical (right) adapted from [5].

to mass values, and subsequently, distance-specific emission rates were calculated and presented as milligrams per kilometer. With this approach, the sample collection on tubes would be cumulative meaning that the real-time (second-by-second) data was not obtained. Therefore, the average concentrations determined may be biased. To address this, a proprietary on-board constant volume sampling and proportional flow dilution system together with a geofencing system, that automatically switched between different sample tubes at pre-set geographical points on the test cycle, enabled an understanding of the breakdown of emissions between different driving modes [5]. For this work, the driving modes and respective geofences were cold-start (CS), urban (U), rural (R), and motorway (M). An example of test route geofencing is shown on the right of Figure 4. The array of tubes, with rows for geofenced segments, and columns for different sample tubes (VOCs, CH_2O, N_2O, etc) are shown on the left of Figure 4 [5].

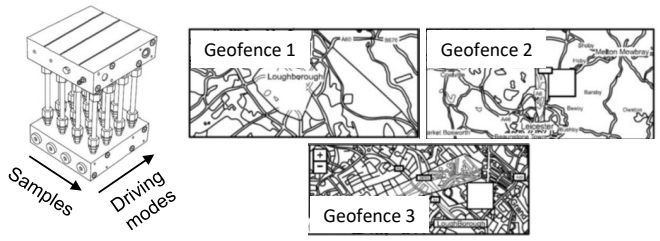

Figure 4: Sampling tube array for the proprietary system (left) and an example geofencing of the test routes (right) adapted from [5].

EXPERIMENTAL METHODOLOGY

FUELS

The bespoke fuels were carefully designed to be market representative and meet the EN228 specifications [53] with the properties shown in Table 3. They were made from refinery streams blended together by Coryton Fuels. The E0 fuel represents a gasoline blend with 0 %v/v ethanol and the E10 fuel represents 10 %v/v ethanol in refinery-based market gasoline. Both fuels were tested on the laboratory-based engine and all four vehicles.

The fuel composition shown in Table 3 was derived from the fuel supplier's detailed hydrocarbon analysis performed according to the ASTM D6730 standard [64]. This test method determines individual component concentrations in the range of 0.01 % to approximately 30 % by mass, however, for oxygenate components such as methanol, ethanol, and methyl tert-butyl ether (MTBE), the concentration ranges from 1 % to 30 % by mass. Therefore, the test method's detection of 0.03 %v/v of ethanol for the E0 fuel could be associated with the inherent uncertainty in the ASTM D6730 test during the measurements of the E0 fuel or present in minimal traces from one of the refinery streams.

Table 3: E0 and E10 fuel properties and composition specification.

Property	Unit	E0	E10
RON	-	95.5	95.7
MON	-	85.6	85.2
Density at 15°C	kg/L	0.7429	0.7497
DVPE at 38°C	kPa	67.6	60.6
E70	% vol	27.5	46.5
E100	% vol	49.8	62.1
E150	% vol	86.7	93.8
Net calorific value	MJ/kg	42.83	40.82
n-paraffins	% v/v	9.3	11.8
iso-paraffins	% v/v	43.0	34.2
olefins	% v/v	10.8	8.1
naphthenes	% v/v	4.1	2.3
aromatics	% v/v	32.1	33.3
Oxygenates (ethanol)	% v/v	0.03	10.2

Table 4: Specification of the four cars used in this study.

	Car 1	Car 2	Car 3	Car 4
Model year	2020	2022		
Regulatory stage	Euro 6d-Temp (WLTP)	Euro 6d-Temp-EVAP-ISC (WLTP)		
Vehicle Segment	Medium Car (C)	Multi-purpose Car (M)	Small Car (B)	
Make	Kia	Peugeot	Citroen	Renault
Model	Sportage	2008	C3	Clio
Power (kW)	129.8	96.2	61.1	67.1
Engine capacity (dm^3)	1.591	1.199	1.199	0.999
Mileage (miles)	24332	8101	471	1901
Gearbox	Manual 6 speed	Automatic 8 speed	Manual 5 speed	Manual 6 speed

SINGLE CYLINDER ENGINE

The engine was first warmed up until the coolant temperatures had stabilized, and the tests were carried out at ambient air intake conditions (298 $\pm$ 5 K). The operating conditions were varied between two IMEPs of 2 and 3 bar ($\pm$ 0.20 bar) and two engine speeds of 1100 and 1500 rpm ($\pm$ 10 rpm) whilst at stoichiometry. Across all tests, the median coefficient of variation (CoV) of IMEP was 3 %. The fuel-air equivalence ratio (ϕ) and IMEP were controlled by adjusting the throttle position and injection duration. For each test, the data from 300 consecutive cycles were collected and then averaged. Three runs were performed for each operating condition.

The engine-out emissions results presented are an average of three independent runs collected for 300 consecutive cycles each. The error bars on the results plots represent the maximum and minimum of the respective emission from each run.

REAL DRIVING EMISSIONS

Four small to medium-sized vehicles with Euro 6d-TEMP emissions regulation stages and further descriptors, shown in Table 4, were used in this study. All vehicles were solely powered with a gasoline internal combustion engine (ICE) and none of the vehicles were hybrid with electric drive functionality. The vehicles were selected from four different manufacturers. Three out of the four cars tested had manual gearboxes and the default driver selectable mode was engaged. The vehicles had similar after-treatment system architecture composed of a three-way catalyst (TWC) and a gasoline particulate filter (GPF). Car 1 was an older model vehicle than Cars 2 to 4 and had a greater mileage than the other vehicles which may impact the condition of the after-treatment systems. All vehicles were tested in October 2022. Both fuels were tested in each vehicle and the entire fuel system was flushed before running the tests. The emissions for each vehicle were measured at the tailpipe using both the SEMTECH-LDV PEMS and the proprietary VOCs system.

All the vehicle and fuel combinations were tested on Emissions Analytics' standard EQUA™ Index test cycle which was twice as long and has a wider range of dynamic driving modes compared to the certification real-driving emissions (RDE) test [5]. Furthermore, the EQUA™ route was used as it contained boundary conditions of speed, acceleration, idling, and gradients, therefore providing good repeatability.

A cold-start (CS) phase was included whilst the urban (U), rural (R), and motorway (M) driving modes were conducted with a warm engine. The cold-start emissions were collected in a separate tube. The cold-start phase was conducted in urban-like conditions but with no stop/start scenarios. The end of the cold-start driving condition was determined at a point when the engine temperature reached between 80 - 84 °C and this approach was maintained across all vehicle and fuel combinations. The distances for the cold-start, urban, rural, and motorway conditions were 4.0 miles, 26.6 miles, 11.3 miles, and 38.7 miles, respectively, totaling approximately 80.8 miles on average across all vehicle and fuel combinations. Furthermore, the mean speeds of the cold-start, urban, rural, and motorway conditions were 28 mph, 19 mph, 29 mph, and 65 mph on average across all vehicle and fuel combinations, respectively. The fuel consumption (liters per 100 km) of the vehicles for each fuel during this study is shown in Appendix A. The test route in this study was aimed to replicate real driving conditions in the United Kingdom. The higher speeds on the test were achieved during the motorway condition where the speed limit is 70 mph (112 km/h).

A single test was performed for each vehicle-fuel combination. Prior to commencing each test, the fuel was drained from the tank by pumping it completely out and the new fuel was pumped in. Once the new fuel was put in the vehicle, it was run for 100 miles to be pre-conditioned and exposed to the new fuel. Additionally, for all cars in the study, the vehicles were first run on the E0 and subsequently the E10 fuel.

As the tailpipe exhaust emissions collected through the SEMTECH-LDV PEMS unit were recorded in real-time (1 Hz), the data was divided into respective driving modes based on the geofences. This enabled comparison with VOCs data collected through the Emissions Analytics proprietary VOCs system. The vehicles had an active start/stop system during the testing. This affected the emissions data collected. There were instantaneous peaks of emissions measurements that were anomalous to the test run and were excluded from the PEMS data.

RESULTS AND DISCUSSION

ALDEHYDES

As aldehydes are inherently formed during ethanol's low-temperature oxidation, the impact of ethanol addition in an E10 fuel compared to E0 was investigated. The real-driving emissions using the proprietary VOCs system could distinguish the concentration of exhaust aldehyde emissions at each of the driving segments and this was evaluated across the cars and fuels. Engine-out emissions measurements from the laboratory-based engine data at low load and engine speed conditions were used to corroborate the findings.

Formaldehyde

Across all four vehicles, the tailpipe exhaust formaldehyde emissions were greatest during the cold-start (CS), whereas the lowest was during the motorway (M) driving phase. This trend is consistent for both E0 and E10 as shown in Figures 5 and 6, respectively. These findings agree with the literature since the low combustion and exhaust temperatures, as well as the

longer duration for after-treatment system warm-up, leads to increased formaldehyde emissions at cold-start. During the motorway phase, the temperatures will be sufficiently higher to consume the formaldehyde during combustion and the after-treatment system would eliminate the remainder. The rural (R) and urban (U) driving phases present comparable formaldehyde emissions for both fuels. This is different from the literature as the urban driving segment would experience more stop-and-start scenarios thus reducing the exhaust temperature and leading to greater formaldehyde. This could be because the after-treatment system effectively eliminates formaldehyde emissions at these conditions despite the fluctuation in engine conditions.

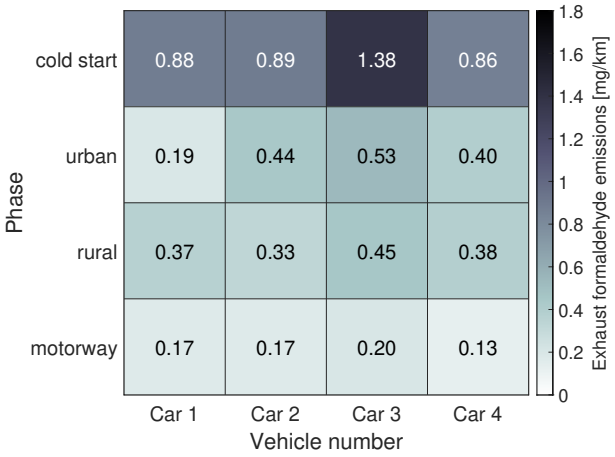

Figure 5: Tailpipe exhaust formaldehyde emissions (mg/km) across the four different vehicles (columns) and driving conditions (rows) with the E0 fuel.

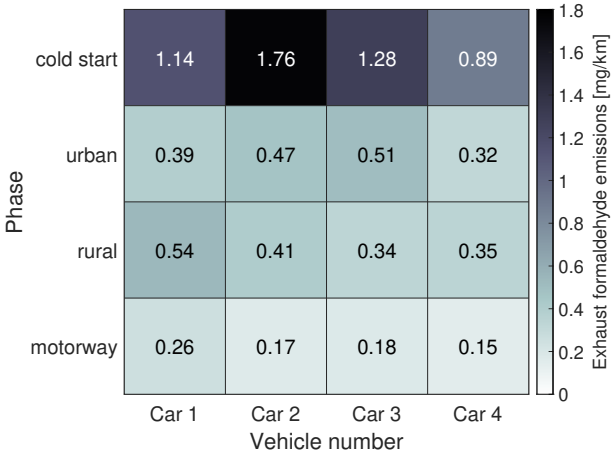

Figure 6: Tailpipe exhaust formaldehyde emissions (mg/km) across the four different vehicles (columns) and driving conditions (rows) with the E10 fuel.

For each of the cars, the relative magnitude of the formaldehyde emissions is similar showing consistency in the testing methods and the effectiveness of the modern emissions treatment systems. For all vehicles, except Car 3, the formaldehyde emissions slightly increased for the E10 fuel compared to E0. For Car 2, the formaldehyde emissions double for the E10 fuel at the cold-start. The moderate increase in formaldehyde emissions is in line with literature findings, particularly as a low-content ethanol fuel was tested [12].

To better understand the impact of the fuel, the engine-out formaldehyde emissions from the laboratory engine at 1100 and 1500 rpm, and 2 and 3 bar are evaluated as presented in Figure 7. Both fuels, E0 and E10 were tested at each of the operating conditions. The error bars present the maximum and minimum readings across the 300 cycles of each of the three repeats.

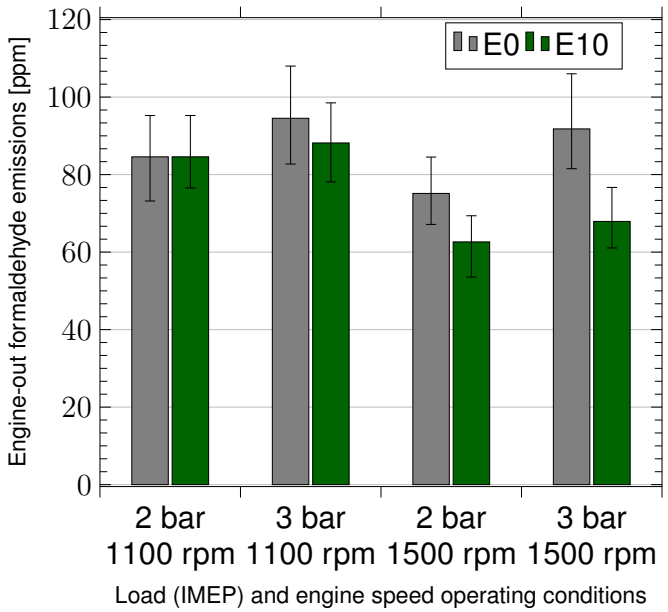

Figure 7: Engine-out formaldehyde emissions for E0 (gray) and E10 (green) at engine speeds of 1100 rpm and 1500 rpm and engine loads of 2 and 3 bar IMEP at stoichiometric conditions. Error bars represent minimum and maximum emissions over three runs of 300 cycles each.

Interestingly, a decrease in engine-out formaldehyde emissions is observed with the E10 fuel for most operating conditions except at 1100 rpm and 2 bar. The decrease is exemplified at the higher speed and load condition suggesting the combustion conditions with E10 were more suitable for formaldehyde consumption. As the ignition timing was early, this may have favored the ethanol combustion leading to higher cylinder temperatures.

Acetaldehyde

Acetaldehyde was detected as an engine-out emission, albeit at low quantities, across all operating conditions and for both E0 and E10 fuels. Interestingly, acetaldehyde emissions were observed even for the E0 fuel. This could be attributed to its formation from non-oxygenate components such as iso-octane, as shown in previous work by the group at the same low speed and load conditions [54]. Iso-octane made up 20 % of the iso-paraffin content for the E0 fuel, whereas only 7 % for the E10 fuel. Figure 8 clearly displays that for both speed and load conditions, the acetaldehyde emissions increase for the E10 fuel. At the lower speed (1100 rpm) conditions, the acetaldehyde emissions increase by approximately 70 %, whereas, at 1500 rpm, the increase is only around 30 %. This suggests the combustion temperatures are low and suitable for acetaldehyde formation at low speed and load conditions as also found by Wallner *et al.* [13]. These observations agree with literature findings [14, 15, 21, 22].

In real-driving scenarios, these conditions can be translated to when the vehicle starts and the engine is not fully warmed up, such as the cold-start (CS) phase, and during urban or rural conditions where the vehicles start/stop more frequently and move at lower speeds.

For all four vehicles, driving segments, and both fuels, tailpipe exhaust acetaldehyde emissions were not detected. As acetaldehyde has been observed in several studies when ethanol is part of the fuel composition, this work suggests that the exhaust after-treatment systems in modern vehicles are capable

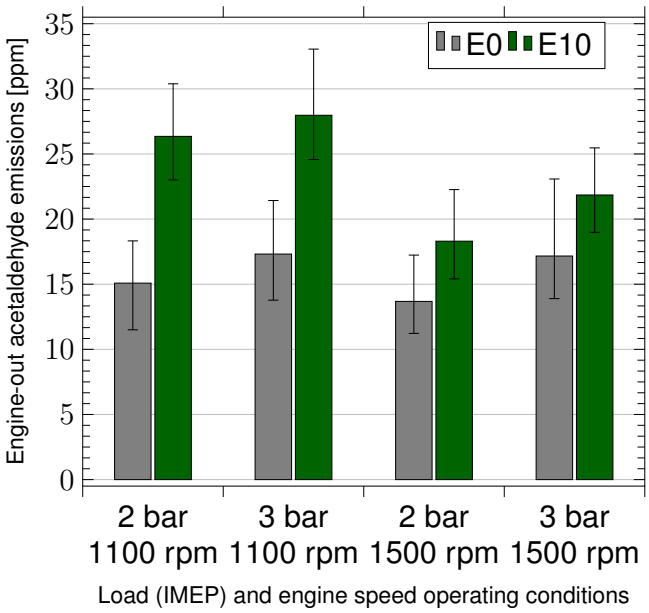

Figure 8: Engine-out acetaldehyde emissions for E0 (gray) and E10 (green) at engine speeds of 1100 and 1500 rpm and engine loads of 2 and 3 bar IMEP at stoichiometric conditions. Error bars represent minimum and maximum emissions over three runs.

of removing the acetaldehyde. Although Bielaczyc *et al.* [65] found that formaldehyde and acetaldehyde were eliminated with approximately equal efficacy in the exhaust after-treatment system of a vehicle with Euro 5 emissions specification, for the Euro 6d-TEMP emissions specification vehicles tested in this study, formaldehyde was detected and acetaldehyde was not.

Agarwal *et al.* [17] found that acetaldehyde emissions were not detectable from gasoline. Other literature also shows that the increase in acetaldehyde engine-out emissions is greater for higher ethanol content in gasoline [15, 23].

Other low carbon number molecules

As acetaldehyde was not detected in the real-driving emissions tests, other molecules with a low number of carbon atoms in the samples collected were investigated. No hydrocarbon molecules with one carbon atom were detected as they were too volatile and would decompose to other molecules. Acetone ($(CH_3)_2CO$) and acetic acid (CH_3COOH) were two recurring molecules across all four driving phases and vehicles. They are both associated with emissions formed from fuels that contain increased oxygenate content. Acetone and acetic acid also pose health and environmental concerns.

The tailpipe exhaust acetone emissions were 5-fold greater for the cold-start than motorway conditions as shown in Figure 9. Similarly, the cold-start acetone emissions were 2 and 4 times greater than rural and urban conditions, respectively. On average, a reduction in acetone emissions is observed with E10 fuel at the cold-start condition across the four vehicles. A reduction in acetone emissions is observed with the E10 fuel at the cold-start conditions for Cars 3 and 4.

For the urban condition, whilst Cars 2 to 4 had an increase in acetone emissions with the E10 fuel, Car 1 had a reduction. At the rural condition, a reduction of an average of 14 % was observed across all four vehicles with the E10 fuel compared to the E0. For the motorway condition, the acetone emissions increased with the E10 fuel for Cars 1 and 2 and decreased for Cars 3 and 4. The rural driving conditions led to twice the tailpipe exhaust acetone emissions than the urban driving conditions for both fuels across all the cars. This distinction between

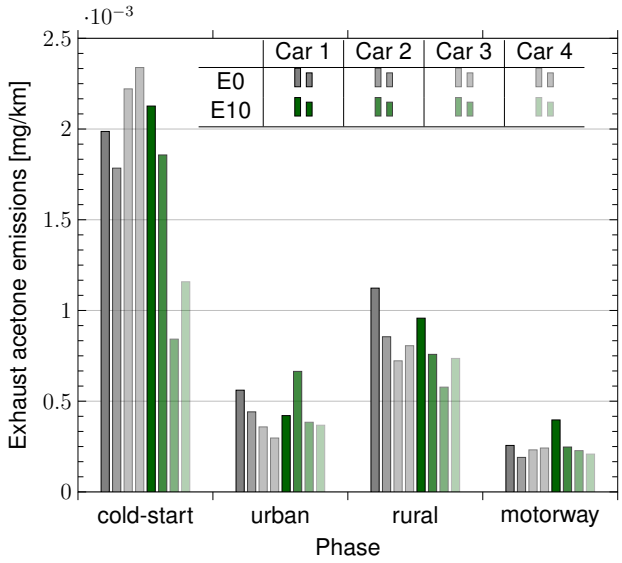

Figure 9: Tailpipe exhaust acetone emissions for E0 (gray) and E10 (green) fuels with four cars (represented by varying shades of each color) across four different driving modes.

urban and rural conditions was not as clear for the tailpipe exhaust formaldehyde emissions. The acetone emissions were not recorded on the AVL FTIR, therefore laboratory-based engine-out emissions data are not available for these emissions.

Zervas *et al.* [28] found that exhaust acetic acid was slightly enhanced from the presence of oxygenated fuel components, such as ethanol. Therefore, the tailpipe exhaust acetic acid emissions were evaluated across the four cars and driving conditions for E0 and E10 as shown in Figure 10. In line with the other emissions evaluated, the cold-start emissions are, on average, at least double the acetic acid emissions for the other conditions. Similarly, the motorway conditions present the lowest acetic acid emissions. These distinct findings emphasize the importance of segregating the real-driving emissions and investigating the impact individually.

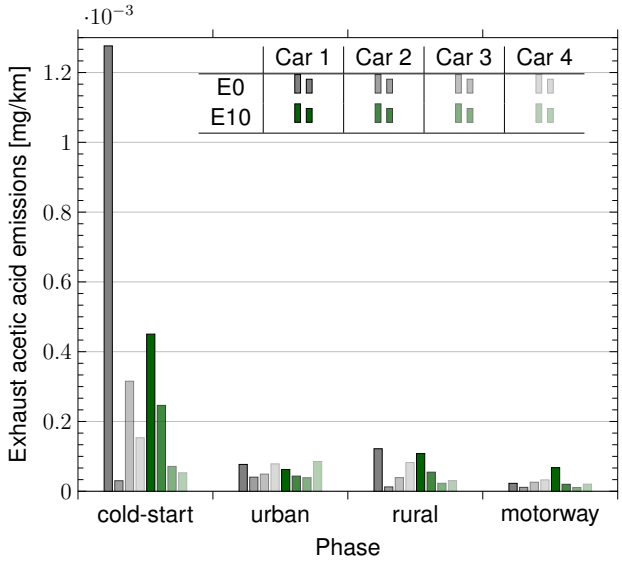

Figure 10: Tailpipe exhaust acetic acid emissions for E0 (gray) and E10 (green) fuels with four cars (represented by varying shades of each color) across four different driving modes.

Contrary to the consistency in tailpipe exhaust emissions amongst the cars found in the previous investigations, there are

significant discrepancies between the cars for acetic acid emissions. This is particularly evident for the cold-start condition with E0 fuel. The significantly greater exhaust tailpipe acetic acid emissions for Car 1 with the E0 fuel during the cold-start conditions may be associated with the higher mileage of the vehicle and thus reduced functionality of the after-treatment system.

ALDEHYDES AND ALCOHOLS

As alcohols are well-known precursors of intermediate aldehydes and the proprietary VOCs system was able to distinctively speciate low carbon atom number alcohols and aldehydes, the correlation between the total tailpipe exhaust alcohol and aldehyde (each up to C_7) was evaluated. C_2 to C_7 alcohols and aldehydes were selected as they constituted a significant proportion of the total respective emissions. As the proprietary VOCs system was used for these measurements, the data for the different driving segments and cars are presented. The results for all 4 cars with the E0 and E10 fuels are shown in Figures 11 and 12, respectively.

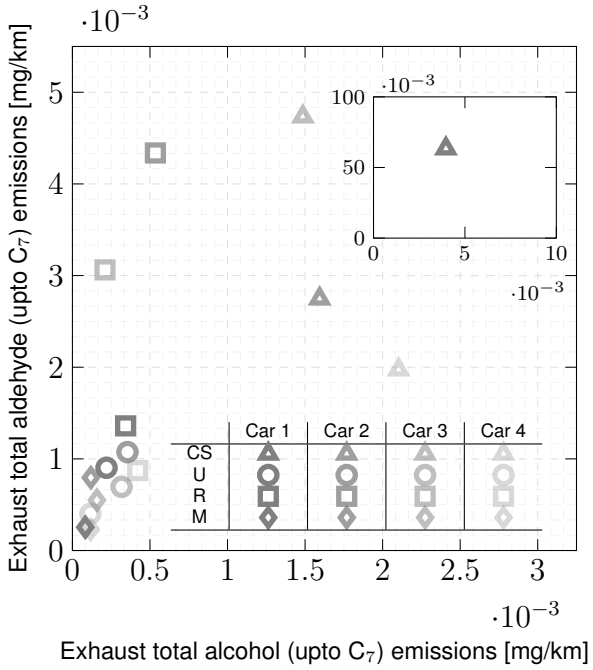

Figure 11: Total tailpipe exhaust aldehyde and alcohol (up to C_7) emissions (mg/km) for all four vehicles (represented by varying shades of gray) with the E0 fuel. Driving phases: cold-start (CS) (triangle), urban (U) (circle), rural (R) (square), and motorway (M) (diamond). Insert plot top right to show anomaly data.

Figure 11 shows that for E0, the total tailpipe exhaust alcohol emissions are lower than the aldehyde emissions, particularly for motorway, rural and urban conditions. For Cars 2 and 3, at the rural driving phase, the aldehyde to alcohol emissions ratio is around 9:1. For the cold-start condition, similar behavior is observed, although the data for the four vehicles is more widely dispersed compared to the other driving conditions. At the cold-start phase, Car 1 presents anomalous data that is significantly greater in both total tailpipe exhaust alcohol and aldehyde emissions. This may be associated with Car 1 being older, having greater mileage, and thus a more used after-treatment system. However, the observed trend remains, with the total aldehyde emissions 10 times greater than the respective total alcohol emissions. These results indicate the intermediate formation of alcohols is lower than aldehyde during the combustion of the hydrocarbons present in the E0 fuel.

Figure 12 with the E10 fuel presents similar behavior to the E0 fuel where the total tailpipe exhaust alcohol and acetaldehyde emissions are within the same ranges. However, compared to the E0 fuel, the ratio of aldehyde to alcohol emissions is significantly lower, especially for the motorway, urban, and rural driving phases. Furthermore, the correlation between alcohol and aldehyde emissions is less prominent for the E10 fuel. The E10 fuel contains 10 %v/v of ethanol content, therefore, the potential for increased unburned alcohol emissions is greater with the E10 fuel than with the E0 fuel. The total aldehyde emissions are not significantly greater for the E10 fuel. This follows the trends observed with the formaldehyde and estimated acetaldehyde tailpipe exhaust emissions found in this investigation.

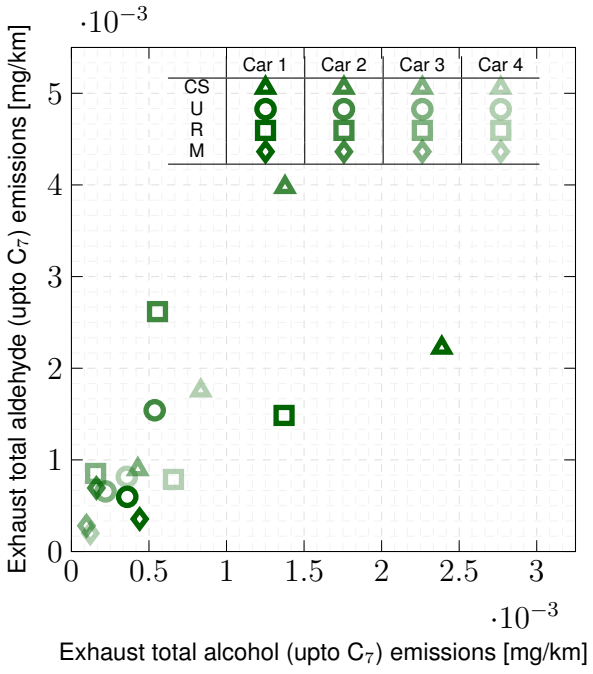

Figure 12: Total tailpipe exhaust aldehyde and alcohol (up to C_7) emissions (mg/km) for all four vehicles (represented by varying shades of green) with the E10 fuel. Driving phases: cold-start (CS) (triangle), urban (U) (circle), rural (R) (square), and motorway (M) (diamond).

BENZALDEHYDE AND TOLUENE

The proprietary VOCs system was capable of detecting tailpipe exhaust benzaldehyde and toluene emissions across all four driving conditions and vehicles. Investigating these harmful pollutants can help better inform future regulatory standards. As toluene is a well-known precursor for benzaldehyde, this analysis would aid the understanding of the impact of the fuel composition on the tailpipe exhaust benzaldehyde and toluene emissions. This data was analyzed for the E0 and E10 fuels as shown in Figures 13 and 14, respectively.

Figure 13 shows that the magnitude of the tailpipe exhaust toluene emissions is significantly greater than the benzaldehyde emissions except for Car 1 at the cold-start conditions. The discrepancy in Car 1's data may be associated with the greater mileage and thus more used after-treatment system leading to lower efficacy in reducing the emissions. On average, the toluene emissions are 20 times greater than benzaldehyde. The toluene emissions originated from the unburned fuel as Zervas *et al.* [33, 66] found that non-aromatic fuel components do not influence the production of toluene in the exhaust.

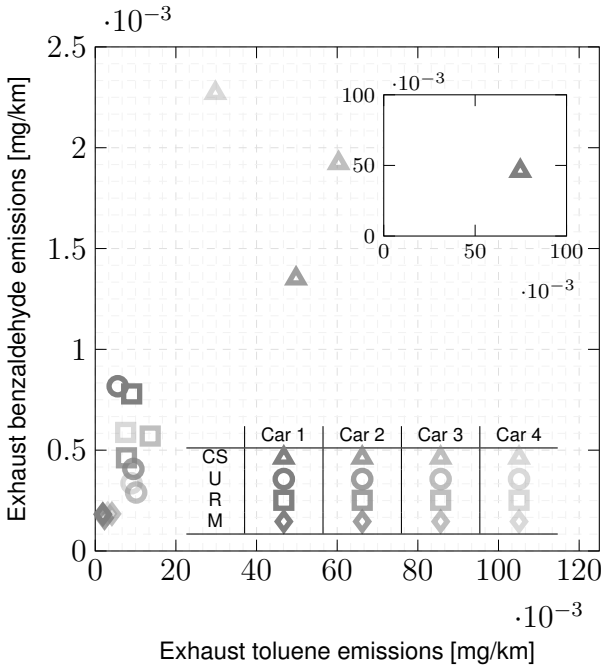

Figure 13: Tailpipe exhaust benzaldehyde and toluene emissions (mg/km) for all four vehicles (represented by varying shades of gray) with the E0 fuel. Driving phases: cold-start (CS) (triangle), urban (U) (circle), rural (R) (square), and motorway (M) (diamond). Insert plot top right to show anomaly data.

Similar to the other detected emissions from the VOCs system, the toluene and benzaldehyde emissions are greatest for cold-start and lowest for motorway conditions. At the motorway driving phase, the toluene and benzaldehyde emissions are approximately 20- and 10-fold lower than at the cold-start conditions, respectively.

There are more consistent levels of exhaust tailpipe toluene and benzaldehyde emissions at the motorway conditions compared to the cold-start. At the latter condition, a multitude of factors such as engine and exhaust after-treatment temperature affect the complex chemistry of toluene oxidation leading to inconsistency amongst the vehicles. Furthermore, across the different driving modes tested ranging from cold-start to motorway, the toluene-to-benzaldehyde ratio decreases from 27 to 16 (except for Car 1). This finding affirms that at low-temperature conditions, the oxidation of toluene to benzaldehyde is less prevalent.

With the E10 fuel, the benzaldehyde to toluene ratio is lower across all driving conditions and vehicles, with this behavior exaggerated for Car 1 at the cold-start condition as shown in Figure 14. Therefore, it is assumed that less of the stable intermediate benzaldehyde was formed from toluene's oxidation. For both fuels, the aromatic content was kept consistent. This could be attributed to the addition of ethanol which leads to a lower combustion mixture temperature as the ethanol-gasoline blended fuel has a higher latent heat of vaporization. However, the literature presents competing results as Zervas *et al.* [66] found low oxygenate content fuels to slightly enhance benzaldehyde formation, whereas Magnusson *et al.* [37] found the formation of benzaldehyde from ethanol was negligible.

For this investigation, on average, the toluene emissions are 34 times greater than the benzaldehyde emissions across the different driving phases and vehicles. Similar to the trends observed with the E0 fuel, the toluene-to-benzaldehyde ratio decreases from 42 to 24 between the cold-start and motorway driving phases. Furthermore, the relative magnitude of tailpipe benzaldehyde and toluene emissions are similar between the E0 and E10 fuels. This is although Fan *et al.* [67] found that ethanol

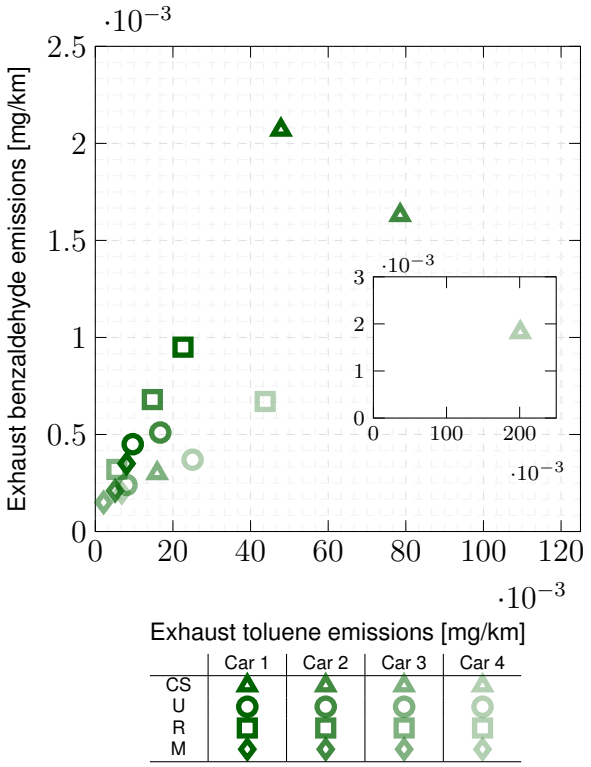

Figure 14: Tailpipe exhaust benzaldehyde and toluene emissions (mg/km) for all four vehicles (represented by varying shades of green) with the E10 fuel. Driving phases: cold-start (CS) (triangle), urban (U) (circle), rural (R) (square), and motorway (M) (diamond). Insert plot top right to show anomaly data.

addition would enhance the reactivity of toluene thus consuming it faster.

NITROUS OXIDE (N_2O)

Given the high global warming potential of N_2O, it is being considered for upcoming regulations, such as the Euro 7 [68]. For this study, the real-driving emissions of N_2O were measured separately in the tubes for each driving phase using the proprietary VOCs system. Therefore, the tailpipe exhaust N_2O emissions are presented for the different driving segments and vehicles with the E0 and E10 fuels, in Figures 15 and 16, respectively.

Figure 15 shows that the cold-start N_2O emissions were 8 times greater than the motorway conditions for both fuels. This behavior is expected, as the cold-start conditions reflect the period during which the exhaust after-treatment experiences catalyst light-off. The literature shows that at these low temperatures, the N_2O emissions are formed as the catalyst surface has not reached a sufficient temperature to completely reduce the NO [49]. These findings attribute the N_2O to be primarily associated with the exhaust after-treatment system and not the fuel, although higher content ethanol-gasoline blends may produce different results.

Figure 15 also shows that the N_2O emissions are approximately 3.5 times greater for rural driving conditions than in the urban phase. These results are similar to the observations made for acetone and acetic acid and different from the formaldehyde and thus predicted acetaldehyde emissions. For the rural driving phase, the greater N_2O formation could be attributed to the reduction of NO by an alkane at higher temperatures in the exhaust after-treatment system as Wang *et al.* [51] reported.

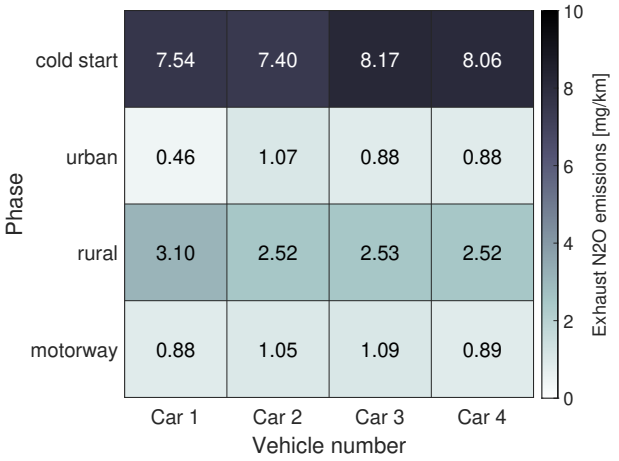

Figure 15: Tailpipe exhaust nitrous oxide N_2O emissions (mg/km) across the four different vehicles (columns) and driving conditions (rows) with the E0 fuel.

Figure 16 shows that the tailpipe exhaust N_2O emissions for the E10 fuel are similar to the E0 fuel for cold-start and rural conditions. Whereas, for urban and motorway conditions, they increased by 27 % and 11 % averaged across the four vehicles, respectively, with the E10 fuel compared to E0 fuel. Nevertheless, for both fuels, the absolute magnitude of N_2O emissions was similar across the four vehicles for each of the driving conditions.

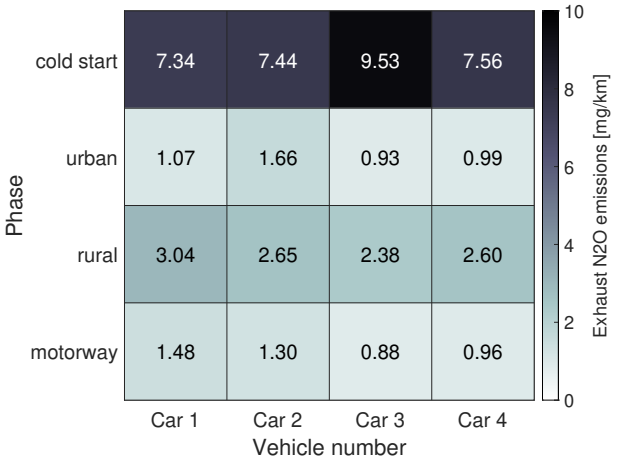

Figure 16: Tailpipe exhaust nitrous oxide N_2O emissions (mg/km) across the four different vehicles (columns) and driving conditions (rows) with the E10 fuel.

As N_2O formation is reported to primarily occur in the exhaust after-treatment system, the emissions from the laboratory-based engine were explored. The engine-out N_2O emissions at 1100 rpm and 1500 rpm and at stoichiometric conditions with a load of 2 bar are shown in Figure 17. Comparing E0 and E10 fuels, there is a marginal increase, although within the error bars. At the higher engine speed condition, the N_2O decreases for both fuels by approximately 30 % and this could be attributed to the increased in-cylinder temperature. However, as the readings are below 10 ppm at engine-out, this affirms that primary N_2O formation occurs in the exhaust after-treatment.

Whilst the N_2O emissions trends are similar to the aldehydes due to their low-temperature formation mechanisms, the opposite would be expected for NO emissions which would constitute a significant proportion of the NOx emissions. Furthermore, the current literature presents conflicting results on the impact of ethanol on NOx emissions. Therefore, the measured tailpipe exhaust NOx was further investigated in this study.

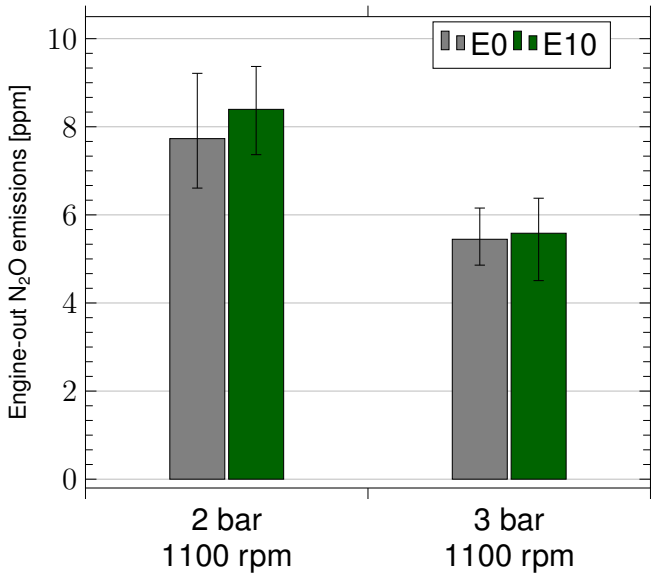

Figure 17: Engine-out N_2O emissions for E0 (gray) and E10 (green) at engine speeds of 1100 and 1500 rpm and engine load of 2 IMEP at stoichiometric conditions. Error bars represent minimum and maximum emissions over three runs.

Additionally, Becker *et al.* [69] found a correlation between N_2O and CO emissions and attributed this to the oxygen availability on the catalyst. However, Graham *et al.* [50] found that N_2O emissions were well correlated with non-methane hydrocarbons (NMHC) and less so with CO emissions. Therefore, the CO emissions that were measured from this study were further investigated.

NITROGEN OXIDE (NO_X)

Figure 18 presents the tailpipe exhaust NOx emissions for the four vehicles at each driving phase. On average, the NOx emissions are greatest at the urban and cold-start and lower for the rural and motorway conditions. At the urban condition, the NOx emissions are consistently greater for the E10 fuel compared to the E0 fuel with an average increase of 185 % across the four vehicles. However, it should be noted that this increase is from very low levels, all vehicles have NOx emissions at less than a third of the very low level mandated in Euro 6 and indeed the proposed value for Euro 7 emissions legislation. Whereas, the opposite behavior is observed for the motorway condition. The formation of NOx is complicated and primarily dependent on the temperatures, although the fuel chemistry can also play a role. Tests by O'Driscoll *et al.* also found that the NOx emissions were higher during urban driving than motorway conditions by 200 % when measured using similar PEMS equipment [46].

These findings are key to understanding the location of the NOx emissions and the resulting public exposure. The high NOx emissions at the urban and cold-start conditions could negatively affect public health in densely populated areas.

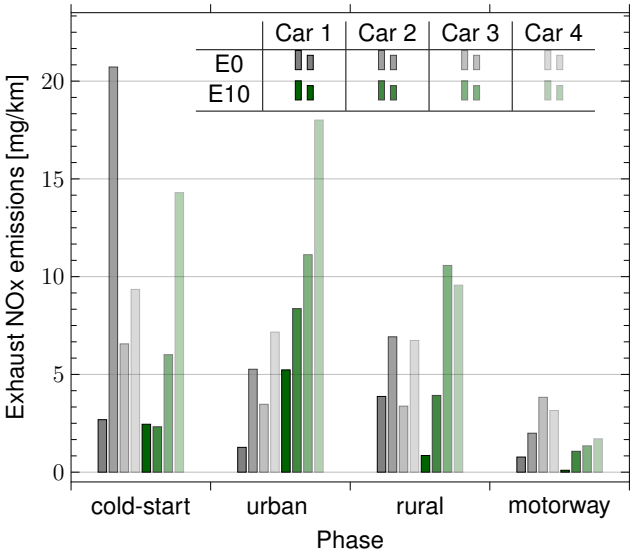

Figure 18: Tailpipe exhaust NOx emissions for E0 (gray) and E10 (green) fuels with four cars (represented by varying shades of each color) across four different driving modes.

CARBON MONOXIDE (CO)

Generally, the addition of ethanol content to gasoline would reduce the CO emissions due to the increased oxygen availability. However, the literature also shows that an increase in CO emissions is observed at lower temperatures, such as the cold-start condition, which could be prolonged with ethanol content [52]. Therefore, the tailpipe exhaust CO emissions from the real-driving conditions, collected by the PEMS, were evaluated. Figure 19 shows the CO emissions comparing E0 and E10 for the four vehicles and driving conditions.

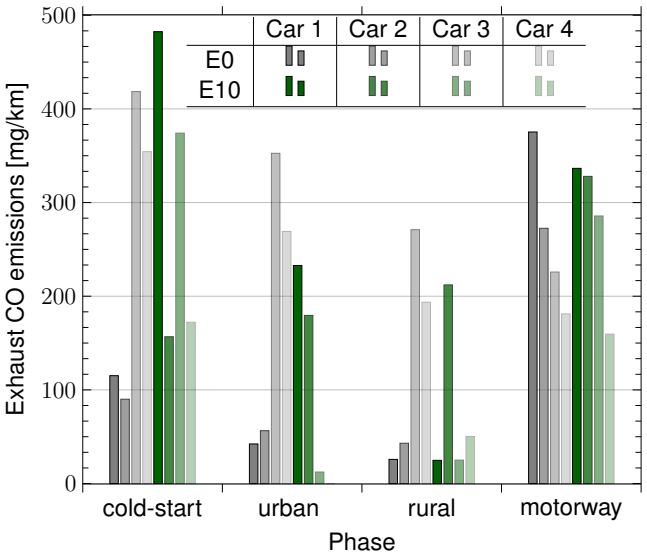

Figure 19: Tailpipe exhaust CO emissions for E0 (gray) and E10 (green) fuels with four cars (represented by varying shades of each color) across four different driving modes.

The CO emissions are greater for the cold-start and motorway conditions compared to the urban and rural. At the motorway conditions, Cars 1 and 4 display a reduction in CO with the E10 fuel compared to E0, whereas Cars 2 and 3 display the opposite. For the cold-start, urban, and rural conditions, the difference in CO emissions between vehicles and fuels is inconsistent, therefore a trend cannot be observed. This may be attributed to the low ethanol content in the fuel and more significant changes could be observed with increased ethanol content.

In comparison to N_2O, no obvious correlation is observed between N_2O and CO from this study. The tailpipe exhaust CO_2 emissions collected on the PEMS are reviewed in the following section.

CARBON DIOXIDE (CO_2)

Generally, the CO_2 emissions with the E0 fuel were higher for vehicles with larger engine size and power (Cars 1 and 2), except for the rural driving condition. The results also present a consistent decrease in CO_2 emissions by an average of 21 % lower for E10 compared to E0 fuel. The greater reductions were observed for cold-start and rural conditions. The E0 fuel results agree with the findings of O'Driscoll *et al.* [46] that CO_2 savings could be made by downsizing gasoline engines, however, no such trend was found in the E10 emissions.

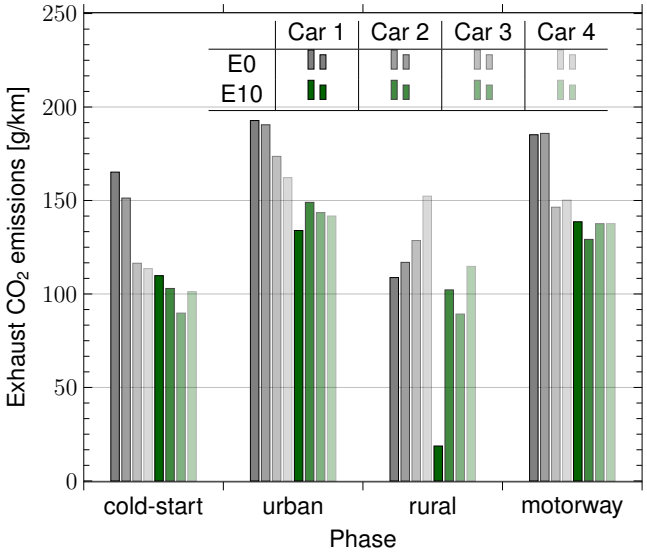

Figure 20: Tailpipe exhaust CO_2 emissions for E0 (gray) and E10 (green) fuels with four cars (represented by varying shades of each color) across four different driving modes.

CONCLUSIONS

This study investigated the impact of ethanol addition to gasoline on several current and to-be regulated, and unregulated emissions. Two fuels, E0 and E10, were tested in four 2020 to 2022 model-year vehicles with Euro 6d-Temp emissions specifications and the real-driving emissions were measured using the PEMS and a Proprietary VOCs system developed by Emissions Analytics. The latter novel system could individually identify hundreds of hydrocarbons and volatile organic compounds that would otherwise be lumped as THC in conventional RDE tests. The two fuels were also tested in a single-cylinder GDI-SI engine and the engine-out emissions were measured using FTIR spectroscopy to corroborate the RDE findings. This study found:

- 14 % increase in tailpipe exhaust formaldehyde emissions for E10 compared to E0 with the greatest proportion and rate of increase between E0 and E10 at the cold-start conditions. This slight increase in formaldehyde due to ethanol addition is in agreement with the literature. However, engine-out formaldehyde emissions decreased for low speed and load conditions.
- Interestingly, tailpipe exhaust acetaldehyde emissions were below the detectable threshold limit across the different

driving segments and cars for both E0 and E10 fuels. This finding is contrasting to literature, however, data from real-driving emissions are often lumped together across the whole drive cycle. Engine-out acetaldehyde emissions increased for E10 compared to E0.

- Tailpipe exhaust acetone emissions were consistent amongst the vehicles and driving conditions. They were 5-fold and 2-fold higher in cold-start and rural in comparison to motorway conditions. Acetone emissions were in the same range for both E0 and E10 fuels.
- Tailpipe exhaust acetic acid emissions were less consistent among vehicles, however, the general trend of driving segments was observed. Acetic acid emissions were in the same range for both E0 and E10 fuels.
- For both fuels, the toluene emissions are greater than benzaldehyde. The toluene-to-benzaldehyde ratio decreases from cold-start to motorway conditions, suggesting that more toluene gets oxidized at higher combustion and exhaust temperatures.
- The tailpipe exhaust N_2O emissions were measured using the VOCs system. As N_2O forms at lower temperatures, the cold-start emissions were 8 times greater than motorway conditions. A significant proportion of N_2O was formed at cold-start. Rural driving conditions had distinctly greater emissions than urban. Whilst the N_2O emissions were similar for the E0 and E10 fuels during the cold-start and rural conditions, they increased with the E10 fuel for the urban and motorway conditions. The N_2O formation appeared to be more dependent on the exhaust after-treatment system.
- No correlation between N_2O and CO was observed. The CO emissions were inconsistent between the fuels and driving conditions across all four vehicles.
- The NOx emissions consistently increased by approximately 185 % on average across the four vehicles between the E0 and E10 fuels at the urban condition. However, at the motorway conditions, the NOx emissions decreased for the E10 fuel for all vehicles tested. These increases are from very low baselines and NOx emissions from all vehicles and fuels tested remained at least 60 % lower than Euro 6 and proposed Euro 7 mandated levels.
- CO_2 emissions consistently decreased across all driving conditions and for all four vehicles with the E10 compared to the E0 fuel. This behavior was accentuated by the cold-start and rural conditions.
- From the real-driving emissions measured in this study, the formaldehyde, low carbon number alcohols and aldehydes, benzaldehyde, toluene, acetone, acetic acid, N_2O, and NOx exhibited lower emissions during the motorway condition. Whereas, for the CO and CO_2 emissions, the motorway conditions led to comparable results with the other driving segments.
- This study presents the impact of fuel composition change on unregulated emissions and highlights the necessity to include these harmful pollutants in legislation with increasing renewable fuel content.

This study shows the importance of having a standardized test comparing known fuel compositions. Furthermore, a significant proportion of the emissions are formed at the cold-start condition and this effect may be weakened when combined with the overall drive cycle.

References

[1] R. Sarwal, S. Kumar, A. Mehta, A. Varadan, S. K. Singh, S. Ramakumar, and R. Mathai, "Ethanol blending in India - 2020-25 Roadmap," *Report of the Expert Committee, Government of India*, 2021.

[2] "Directive (EU) 2018/2001 - the promotion of the use of energy from renewable sources," *European Parliament and of the council*, 2018.

[3] D. Turner, H. Xu, R. F. Cracknell, V. Natarajan, and X. Chen, "Combustion performance of bio-ethanol at various blend ratios in a gasoline direct injection engine," *Fuel*, vol. 90, no. 5, pp. 1999–2006, 2011. doi: 10.1016/j.fuel.2010.12.025.

[4] K. Senecal and F. Leach, *Racing Toward Zero: The Untold Story of Driving Green*. SAE International, 2021.

[5] N. Molden, "Innovative emissions measurement and perspective on future tailpipe regulation : Real-world measurement and role of VOCs and N_2O emissions," *Johnson Matthey Technology Review*, Oct. 2022. doi: 10.1595/205651323x16650512926820.

[6] M. Li, Q. Zhang, B. Zheng, D. Tong, Y. Lei, F. Liu, C. Hong, S. Kang, L. Yan, Y. Zhang, Y. Bo, H. Su, Y. Cheng, and K. He, "Persistent growth of anthropogenic non-methane volatile organic compound (NMVOC) emissions in China during 1990–2017: Drivers, speciation and ozone formation potential," *Atmospheric Chemistry and Physics*, vol. 19, no. 13, pp. 8897–8913, 2019. doi: 10.5194/acp-19-8897-2019.

[7] B. T. P. Thera, P. Dominutti, F. Öztürk, T. Salameh, S. Sauvage, C. Afif, B. Çetin, C. Gaimoz, M. Keleş, S. Evan, and A. Borbon, "Composition and variability of gaseous organic pollution in the port megacity of Istanbul: Source attribution, emission ratios, and inventory evaluation," *Atmospheric Chemistry and Physics*, vol. 19, no. 23, pp. 15 131–15 156, 2019. doi: 10.5194/acp-19-15131-2019.

[8] Y. Liu, M. Song, X. Liu, Y. Zhang, L. Hui, L. Kong, Y. Zhang, C. Zhang, Y. Qu, J. An, D. Ma, Q. Tan, and M. Feng, "Characterization and sources of volatile organic compounds (VOCs) and their related changes during ozone pollution days in 2016 in Beijing, China," *Environmental Pollution*, vol. 257, p. 113 599, 2020. doi: 10.1016/j.envpol.2019.113599.

[9] "Road transport: Reducing CO_2 emissions from vehicles," *European Commission*, 2023.

[10] A. K. Agarwal and N. N. Mustafi, "Real-world automotive emissions: Monitoring methodologies, and control measures," *Renewable and Sustainable Energy Reviews*, vol. 137, p. 110 624, 2021. doi: 10.1016/j.rser.2020.110624.

[11] "Substances listed in the Fifteenth Report on Carcinogens," *U.S. Department of Health and Human Services (HHS) National Toxicology Program*, 2021.

[12] L. A. Graham, S. L. Belisle, and C.-L. Baas, "Emissions from light duty gasoline vehicles operating on low blend ethanol gasoline and E85," *Atmospheric Environment*, vol. 42, no. 19, pp. 4498–4516, 2008. doi: 10.1016/j.atmosenv.2008.01.061.

[13] T. Wallner and R. Frazee, "Study of regulated and non-regulated emissions from combustion of gasoline, alcohol fuels and their blends in a DI-SI engine," *SAE Technical Papers*, 2010. doi: 10.4271/2010-01-1571.

[14] M. Clairotte, T. Adam, A. Zardini, U. Manfredi, G. Martini, A. Krasenbrink, A. Vicet, E. Tournié, and C. Astorga, "Effects of low temperature on the cold start gaseous emissions from light-duty vehicles fuelled by ethanol-blended gasoline," *Applied Energy*, vol. 102, pp. 44–54, 2013. doi: 10.1016/j.apenergy.2012.08.010.

[15] D. Jin, K. Choi, C.-L. Myung, Y. Lim, J. Lee, and S. Park, "The impact of various ethanol-gasoline blends on particulates and unregulated gaseous emissions characteristics from a spark ignition direct injection (SIDI) passenger vehicle," *Fuel*, vol. 209, pp. 702–712, 2017. doi: 10.1016/j.fuel.2017.08.063.

[16] G. Karavalakis, T. D. Durbin, M. Shrivastava, Z. Zheng, M. Villela, and H. Jung, "Impacts of ethanol fuel level on emissions of regulated and unregulated pollutants from a fleet of gasoline light-duty vehicles," *Fuel*, vol. 93, pp. 549–558, 2012. doi: 10.1016/j.fuel.2011.09.021.

[17] A. K. Agarwal, P. C. Shukla, J. G. Gupta, C. Patel, R. K. Prasad, and N. Sharma, "Unregulated emissions from a gasohol (E5, E15, M5, and M15) fuelled spark ignition engine," *Applied Energy*, vol. 154, pp. 732–741, 2015. doi: 10.1016/j.apenergy.2015.05.052.

[18] J. Yang, P. Roth, T. Durbin, and G. Karavalakis, "Impacts of gasoline aromatic and ethanol levels on the emissions from GDI vehicles: Part 1. influence on regulated and gaseous toxic pollutants," *Fuel*, vol. 252, pp. 799–811, 2019. doi: 10.1016/j.fuel.2019.04.143.

[19] S. Cheng, D. Kang, A. Fridlyand, S. S. Goldsborough, C. Saggese, S. Wagnon, M. J. McNenly, M. Mehl, W. J. Pitz, and D. Vuilleumier, "Autoignition behavior of gasoline/ethanol blends at engine-relevant conditions," *Combustion and Flame*, vol. 216, pp. 369–384, 2020. doi: 10.1016/j.combustflame.2020.02.032.

[20] S. M. Sarathy, P. Oßwald, N. Hansen, and K. Kohse-Höinghaus, "Alcohol combustion chemistry," *Progress in Energy and Combustion Science*, vol. 44, pp. 40–102, 2014. doi: 10.1016/j.pecs.2014.04.003.

[21] G. Karavalakis, D. Short, D. Vu, R. L. Russell, A. Asa-Awuku, H. Jung, K. C. Johnson, and T. D. Durbin, "The impact of ethanol and iso-butanol blends on gaseous and particulate emissions from two passenger cars equipped with spray-guided and wall-guided direct injection SI (spark ignition) engines," *Energy*, vol. 82, pp. 168–179, 2015. doi: 10.1016/j.energy.2015.01.023.

[22] S. Puricelli, S. Casadei, T. Bellin, S. Cernuschi, D. Faedo, G. Lonati, T. Rossi, and M. Grosso, "The effects of innovative blends of petrol with renewable fuels on the exhaust emissions of a GDI Euro 6d-TEMP car," *Fuel*, vol. 294, p. 120 483, 2021. doi: 10.1016/j.fuel.2021.120483.

[23] J.-F. Fortune, P. Cologon, P. Hayrault, M. Heninger, J. Leprovost, J. Lemaire, P. Anselmi, and M. Matrat, "Impact of fuel ethanol content on regulated and non-regulated emissions monitored by various analytical techniques over flex-fuel and conversion kit applications," *Fuel*, vol. 334, p. 126 669, 2023. doi: 10.1016/j.fuel.2022.126669.

[24] "Workplace exposure standards for airborne contaminants," *Safe Work Australia*, 2022.

[25] F. L. Dryer and K. Brezinsky, "A flow reactor study of the oxidation of n-octane and iso-octane," *Combustion Science and Technology*, vol. 45, pp. 199–212, 3-4 Feb. 2007. doi: 10.1080/00102208608923850.

[26] S. Poulopoulos, D. Samaras, and C. Philippopoulos, "Regulated and unregulated emissions from an internal combustion engine operating on ethanol-containing fuels," *Atmospheric Environment*, vol. 35, no. 26, pp. 4399–4406, 2001. doi: 10.1016/s1352-2310(01)00248-5.

[27] F. Battin-Leclerc, A. Konnov, J. Jaffrezo, and M. Legrand, "Modelling of the formation of light acids in propane flames," English, in *Proceedings of the 3rd European Combustion Meeting, ECM2007*, 2007.

[28] E. Zervas, X. Montagne, and J. Lahaye, "C1 - C5 organic acid emissions from an SI engine: Influence of fuel and air/fuel equivalence ratio," *Environmental Science & Technology*, vol. 35, no. 13, pp. 2746–2751, 2001. doi: 10.1021/es000237v.

[29] N. Leplat and J. Vandooren, "Numerical and experimental study of the combustion of acetic acid in laminar premixed flames," *Combustion and Flame*, vol. 159, no. 2, pp. 493–499, 2012. doi: 10.1016/j.combustflame.2011.08.007.

[30] M. Christensen and A. A. Konnov, "Laminar burning velocity of acetic acid + air flames," *Combustion and Flame*, vol. 170, pp. 12–29, 2016. doi: 10.1016/j.combustflame.2016.05.007.

[31] A. Andersen, "Final report on the safety assessment of benzaldehyde," *International Journal of Toxicology*, vol. 25, SUPPL. 1 2006. doi: 10.1080/10915810600716612.

[32] P. Dagaut, G. Pengloan, and A. Ristori, "Oxidation, ignition and combustion of toluene: Experimental and detailed chemical kinetic modeling," *Physical Chemistry Chemical Physics*, vol. 4, 10 2002. doi: 10.1039/b110282f.

[33] E. Zervas, "Formation of oxygenated compounds from isooctane/toluene flames," *Energy & Fuels*, vol. 19, no. 5, pp. 1865–1872, 2005. doi: 10.1021/ef050059x.

[34] G. da Silva and J. W. Bozzelli, "Benzoxyl radical decomposition kinetics: Formation of benzaldehyde + H, phenyl + CH_2O, and benzene + HCO," *The Journal of Physical Chemistry A*, vol. 113, no. 25, pp. 6979–6986, 2009. doi: 10.1021/jp902458d.

[35] E. Zervas, X. Montagne, and J. Lahaye, "Emission of alcohols and carbonyl compounds from a spark ignition engine. influence of fuel and air/fuel equivalence ratio," *Environmental Science & Technology*, vol. 36, no. 11, pp. 2414–2421, 2002. doi: 10.1021/es010265t.

[36] S. Manzetti and O. Andersen, "A review of emission products from bioethanol and its blends with gasoline. background for new guidelines for emission control," *Fuel*, vol. 140, pp. 293–301, 2015. doi: 10.1016/j.fuel.2014.09.101.

[37] R. Magnusson, C. Nilsson, and B. Andersson, "Emissions of aldehydes and ketones from a two-stroke engine using ethanol and ethanol-blended gasoline as fuel," *Environmental Science & Technology*, vol. 36, no. 8, pp. 1656–1664, 2002. doi: 10.1021/es010262g.

[38] E. Zervas, X. Montagne, and J. Lahaye, "Emissions of regulated pollutants from a spark ignition engine. influence of fuel and air/fuel equivalence ratio," *Environmental Science & Technology*, vol. 37, no. 14, pp. 3232–3238, 2003. doi: 10.1021/es026321n.

[39] H. Oh, C. Bae, and K. Min, "Spray and combustion characteristics of ethanol blended gasoline in a spray-guided DISI engine under lean stratified operation," *SAE Technical Papers*, pp. 213–222, 2010. doi: 10.4271/2010-01-2152.

[40] P. Bielaczyc, A. Szczotka, and J. Woodburn, "The effect of various petrol-ethanol blends on exhaust emissions and fuel consumption of an unmodified light-duty SI vehicle," *SAE Technical Papers*, 2011. doi: 10.4271/2011-24-0177.

[41] R. Suarez-Bertoa, A. Zardini, H. Keuken, and C. Astorga, "Impact of ethanol containing gasoline blends on emissions from a flex-fuel vehicle tested over the Worldwide Harmonized Light duty Test Cycle (WLTC)," *Fuel*, vol. 143, pp. 173–182, 2015. doi: 10.1016/j.fuel.2014.10.076.

[42] B. Masum, H. Masjuki, M. Kalam, I. Rizwanul Fattah, S. Palash, and M. Abedin, "Effect of ethanol–gasoline blend on NOx emission in SI engine," *Renewable and Sustainable Energy Reviews*, vol. 24, pp. 209–222, 2013. doi: 10.1016/j.rser.2013.03.046.

[43] Z. Zhang, J. Hu, D. Tan, J. Li, F. Jiang, X. Yao, D. Yang, Y. Ye, Z. Zhao, and G. Yang, "Multi-objective optimization of the three-way catalytic converter on the combustion and emission characteristics for a gasoline engine," *Energy*, vol. 277, p. 127 634, 2023. doi: 10.1016/j.energy.2023.127634.

[44] G. Najafi, B. Ghobadian, T. Tavakoli, D. Buttsworth, T. Yusaf, and M. Faizollahnejad, "Performance and exhaust emissions of a gasoline engine with ethanol blended gasoline fuels using artificial neural network," *Applied Energy*, vol. 86, no. 5, pp. 630–639, 2009. doi: 10.1016/j.apenergy.2008.09.017.

[45] I. Schifter, L. Diaz, R. Rodriguez, J. Gómez, and U. Gonzalez, "Combustion and emissions behavior for ethanol–gasoline blends in a single cylinder engine," *Fuel*, vol. 90, no. 12, pp. 3586–3592, 2011, Environmental Modeling of Catalytic Reactions in the Oil Refining Industry. doi: 10.1016/j.fuel.2011.01.034.

[46] R. O'Driscoll, M. E. Stettler, N. Molden, T. Oxley, and H. M. ApSimon, "Real world CO_2 and NOx emissions from 149 Euro 5 and 6 diesel, gasoline, and hybrid passenger cars," *Science of The Total Environment*, vol. 621, pp. 282–290, 2018. doi: 10.1016/j.scitotenv.2017.11.271.

[47] T. Huai, T. D. Durbin, J. Wayne Miller, and J. M. Norbeck, "Estimates of the emission rates of nitrous oxide from light-duty vehicles using different chassis dynamometer test cycles," *Atmospheric Environment*, vol. 38, no. 38, pp. 6621–6629, 2004. doi: 10.1016/j.atmosenv.2004.07.007.

[48] I. Mejía-Centeno, A. Martínez-Hernández, and G. A. Fuentes, "Effect of low-sulfur fuels upon NH_3 and N_2O emission during operation of commercial three-way catalytic converters," *Topics in Catalysis*, vol. 42-43, pp. 381–385, 1-4 May 2007. doi: /10.1007/s11244-007-0210-2.

[49] T. Wallington and P. Wiesen, "N_2O emissions from global transportation," *Atmospheric Environment*, vol. 94, pp. 258–263, 2014. doi: 10.1016/j.atmosenv.2014.05.018.

[50] L. A. Graham, S. L. Belisle, and P. Rieger, "Nitrous oxide emissions from light duty vehicles," *Atmospheric Environment*, vol. 43, no. 12, pp. 2031–2044, 2009. doi: 10.1016/j.atmosenv.2009.01.002.

[51] X. Wang, J. Gao, Z. Chen, H. Chen, Y. Zhao, Y. Huang, and Z. Chen, "Evaluation of hydrous ethanol as a fuel for internal combustion engines: A review," *Renewable Energy*, vol. 194, pp. 504–525, 2022. doi: 10.1016/j.renene.2022.05.132.

[52] R. Suarez-Bertoa and C. Astorga, "Impact of cold temperature on Euro 6 passenger car emissions," *Environmental Pollution*, vol. 234, pp. 318–329, 2018. doi: 10.1016/j.envpol.2017.10.096.

[53] "Automotive fuels-unleaded petrol-requirements and test methods," *European Commission - European Committee for Standardization*, 2008.

[54] V. Shankar and F. Leach, "Effects of oxygenate and aromatic content on engine-out aldehyde emissions from pure, binary, and ternary mixtures of ethanol, toluene, and iso-octane," in *JSAE/SAE Powertrains, Energy and Lubricants International meeting*, SAE International, Sep. 2023.

[55] SEMTECH, "SEMTECH DS+ module specifications," *SEMTECH®*, 2023.

[56] M. Weiss, P. Bonnel, J. Kühlwein, A. Provenza, U. Lambrecht, S. Alessandrini, M. Carriero, R. Colombo, F. Forni, G. Lanappe, P. L. Lijour, U. Manfredi, F. Montigny, and M. Sculati, "Will Euro 6 reduce the NOx emissions of new diesel cars? – insights from on-road tests with portable emissions measurement systems (PEMS)," *Atmospheric Environment*, vol. 62, pp. 657–665, Dec. 2012. doi: 10.1016/j.atmosenv.2012.08.056.

[57] R. O'Driscoll, H. M. Simon, T. Oxley, N. Molden, M. E. Stettler, and A. Thiyagarajah, "A Portable Emissions Measurement system (PEMS) study of NOx and primary NO_2 emissions from Euro 6 diesel passenger cars and comparison with COPERT emission factors," *Atmospheric Environment*, vol. 145, pp. 81–91, 2016. doi: 10.1016/j.atmosenv.2016.09.021.

[58] "Field testing and portable emission measurement systems," *Code of Federal Regulations - Title 40/Chapter 1/Subchapter U/Part 1065/Subchapter J - U.S. Environmental Protection Agency*, 2023.

[59] M. Kousoulidou, G. Fontaras, L. Ntziachristos, P. Bonnel, Z. Samaras, and P. Dilara, "Use of portable emissions measurement system (PEMS) for the development and validation of passenger car emission factors," *Atmospheric Environment*, vol. 64, pp. 329–338, 2013. doi: 10.1016/j.atmosenv.2012.09.062.

[60] N. Molden and D. Booker, "Apparatus and method for sampling an exhaust gas," 2022.

[61] Sepsolve, "INSIGHT®- outstanding performance for routine GC×GC applications," *Sepsolve Analytical*, 2023.

[62] Markes, "Markes International launches world's first range of hydrogen-certified, multi-gas enabled thermal desorption instruments," *Markes International*, 2023.

[63] Agilent, "Analytical HPLC systems - agilent 1220 Infinity II Liquid Chromatography," *Aglient*, 2023.

[64] "Standard test method for determination of individual components in spark ignition engine fuels by 100-metre capillary (with precolumn) high-resolution gas chromatography 1," *ASTM D6730*, 2021. doi: 10.1520/d6730-21.

[65] P. Bielaczyc, J. Woodburn, D. Klimkiewicz, P. Pajdowski, and A. Szczotka, "An examination of the effect of ethanol–gasoline blends' physicochemical properties on emissions from a light-duty spark ignition engine," *Fuel Processing Technology*, vol. 107, pp. 50–63, 2013, Selected Papers from the Eleventh International Conference on Combustion and Energy Utilization (11th ICCEU). doi: 10.1016/j.fuproc.2012.07.030.

[66] E. Zervas, X. Montagne, and J. Lahaye, "Influence of fuel and air/fuel equivalence ratio on the emission of hydrocarbons from a si engine. 2. formation pathways and modelling of combustion processes," *Fuel*, vol. 83, no. 17, pp. 2313–2321, 2004. doi: 10.1016/j.fuel.2004.06.028.

[67] Q. Fan, Z. Wang, Y. Qi, S. Liu, and X. Sun, "Research on ethanol and toluene's synergistic effects on auto-ignition and pressure dependences of flame speed for gasoline surrogates," *Combustion and Flame*, vol. 222, pp. 196–212, 2020. doi: 10.1016/j.combustflame.2020.08.049.

[68] E. Commission, "Regulation of the European Parliament and of the Council on type-approval of motor vehicles and engines of systems, components, and separate technical units intended for such vehicles, with respect to their emissions and battery durability (Euro 7) and repealing Regulations (EC) No 715/2007 and (EC) No 595/2009," 2022.

[69] K. H. Becker, Lörzer, R. Kurtenbach, P. Wiesen, T. E. Jensen, and T. J. Wallington, "Nitrous oxide (N_2O) emissions from vehicles," *Environmental Science & Technology*, vol. 33, no. 22, pp. 4134–4139, 1999. doi: 10.1021/es9903330.

ACKNOWLEDGMENTS

Varun Shankar acknowledges the scholarship support of The Rhodes Trust. This publication also arises from research funded by the John Fell Oxford University Press Research Fund.

CONTACT INFORMATION

Felix Leach, Associate Professor
Department of Engineering Science, University of Oxford,
Parks Rd, Oxford, United Kingdom, OX1 3PJ

felix.leach@eng.ox.ac.uk

DEFINITIONS, ACRONYMS, ABBREVIATIONS

ϕ	fuel-air equivalence ratio
2,4-DNPH	2,4-dinitrophenyl hydrazine
AA	Acetaldehyde
ASTM	American Society for Testing and Materials
BHP	Brake horsepower
BNC	Berkeley Nucleonics Corporation
CoV	Coefficient of variation
CS	Cold-start condition
DVPE	Dry vapor pressure equivalent
ECD	Electron capture detector
EU	European Union
EVC	Exhaust valve closing
EVO	Exhaust valve opening
E0	10 %v/v ethanol, 90 %v/v gasoline
E10	100 %v/v gasoline
FA	Formaldehyde
FID	Flame ionization detector
FTIR	Fourier Transform Infrared Spectroscopy
GCxGC	Two-dimensional gas chromatography
GDI	Gasoline direct injection
GHG	Greenhouse gas
GPF	Gasoline Particulate Filter
GPS	Global Positioning System
HPLC	High performance liquid chromatography
ICE	Internal combustion engine
IMEP	Indicated mean effective pressure
IVC	Intake valve closing
IVO	Intake valve opening
MON	Motor octane number
M	Motorway condition
PEMS	Portable emissions measuring system
R	Rural condition
RDE	Real-driving emissions
RON	Research Octane Number
RPM	Revolutions per minute
SI	Spark ignition
THC	Total hydrocarbons
TOF-MS	Time-of-flight mass spectrometer
TWC	Three-way catalytic converter
U	Urban condition
USA	United States of America
VOCs	Volatile organic compounds

APPENDIX A

The Appendix presents the fuel consumption of the four vehicles with the E0 and E10 fuels based on this study in Table A.1. The results show that for all vehicles except the Citroen C3 Sense Puretech (Car 3), the fuel consumption improved with the E10 compared to the E0. On average, a 4.8 % reduction in fuel consumption was observed with the greatest reduction seen with the Renault Clio RS Line (Car 4).

Table A.1: Fuel consumption [liters per 100 kilometers (l/100 km)] for each vehicle with the E0 and E10 fuels

Vehicle	E0 (l/100 km)	E10 (l/100 km)
2020 Kia Sportage GT-line ISG	6.98	6.68
2022 Peugeot 2008 GT Premium PureTech	6.05	5.77
2022 Citroen C3 Sense PureTech	5.23	5.39
2022 Renault Clio RS Line TCe	5.07	4.48